Chinese Chemical Letters 34 (2023) 107818

Contents lists available at ScienceDirect

Chinese Chemical Letters

journal homepage: www.elsevier.com/locate/cclet

Spiropyran isomerization triggering ESIPT for visualization of pH fluctuations during oxidative stress in living cells

Jingdong Wang[a], Fangjun Huo[b,*], Yongbin Zhang[b], Caixia Yin[a,*]

[a] Institute of Molecular Science, Key Laboratory of Chemical Biology and Molecular Engineering of Ministry of Education, Shanxi University, Taiyuan 030006, China

[b] Research Institute of Applied Chemistry, Shanxi University, Taiyuan 030006, China

ARTICLE INFO

Article history:
Received 8 June 2022
Revised 5 September 2022
Accepted 9 September 2022
Available online 13 September 2022

Keywords:
pH
Spiropyran isomerization
ESIPT
Reversible
Oxidative stress

ABSTRACT

Intracellular pH homeostasis is foundation of maintaining normal physiological functions. More and more evidences show that intracellular pH fluctuations were usually associated with many diseases (such as cancer, epilepsy and neurodegenerative diseases). It is very important to develop *in situ* real-time determination of pH. In recent years, it has been verified that pH can regulate the isomerization process of spiropyran. Thus, we report a pH fluorescent probe **BSL**, which is a closed loop spiropyran structure by coupling benzothiazole derivatives with indole salts. We utilizes the process of spiropyran isomerization as the trigger of excited state intramolecular proton transfer (ESIPT) effect, and adjust the process of spiropyran isomerization through pH, and then the molecular transformation from enol to ketone (enol: 525 nm, ketone: 677 nm) through the ESIPT effect. This process achieved accurate measurement of pH. The probe **BSL** showed sensitive and reversible fluorescence response to pH *in vitro*. Ultimately, **BSL** was successfully applied to detect pH fluctuations in cell oxidative stress model.

Intracellular pH values, as an important parameter, play a key role in maintaining cellular homeostasis and involve in various cellular biological process, such as cell proliferation and apoptosis, enzyme activity, muscle contraction and ion transport [1–6]. In addition, the pH values are highly inhomogenous at the different loactions in cells, *e.g.*, the pH values of endoplasmic reticulum, lysosome and mitochondria are respectively 5.0–6.5, 4.5–5.0 and 8.0, maintaining collectively the normal physiological function in cells [7–9]. However, lysosomes, as important acidic organelles of digestion and cleaning, not only participate in the degradation of various biological macromolecules (*e.g.*, proteins, lipids, nucleic acids and carbohydrates), but also are responsible for intracellular acidification, transport of substances in different organelles, and so on [10–15]. Abnormal fluctuation pH in lysosomes is closely associated with physiological function in cells and lead to the occurrence of a series of diseases, such as Alzheimer's disease, shock, lysosomal storage disorder and even cancer [16–20]. What is more, oxidative stress is usually characterized by excessive production of reactive oxygen species (ROS), which may lead to disruption of cellular homeostasis to trigger pH fluctuations in lysosomes [21–24]. However, the relationship between LPS-stimulated oxidative stress and pH values fluctuations remains unclear until now. Therefore, in order to accurately monitor the process of pH fluctuations in intracellular under oxidative stress, we urgently need to develop fluorescent probe to accurately detect intracellular pH fluctuations.

Several common methods have been used to measure pH, including acid-base indicator titration, nuclear magnetic resonance, electrochemical method, UV–vis absorption spectrum and fluorescence spectroscopy [25–27]. However, these methods require tedious and complex pretreatment of samples. Especially, these manners needs to destroy cells for the detection of intracellular pH, tissue structures and limits their biological applications. Fluorescence imaging technology, due to its advantages of simple operation, high sensitivity, non-invasive, perfect biocompatibility, real-time monitoring, has a wide application prospect in cell imaging [28–31]. In recent years, a range of pH fluorescent probes have been developed, but there are two limitations that prevent them from being well applied in living cells. The main disadvantage is that these pH probes emit at a shorter wavelength (<650 nm), while the near-infrared region (NIR) with a longer emission wavelength allows for less biologic background fluorescence interference and deeper tissue penetration [32,33]. Next, the Stokes shift of the probes is small (<100 nm). In contrast, large Stokes shift can effectively reduce background interference, with strong penetration,

* Corresponding authors.
E-mail addresses: huofj@sxu.edu.cn (F. Huo), yincx@sxu.edu.cn (C. Yin).

https://doi.org/10.1016/j.cclet.2022.107818
1001-8417/

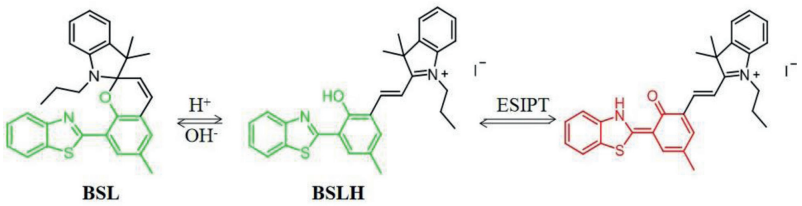

Scheme 1. Mechanism and molecule structure of BSL.

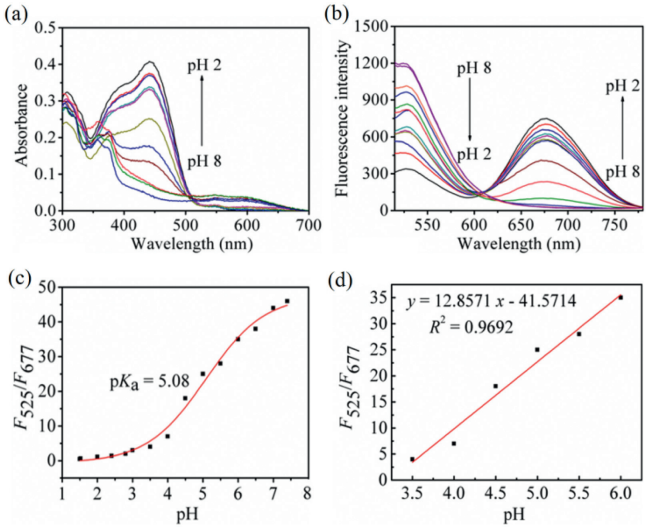

Fig. 1. (a) Absorption spectra change of BSL (10 μmol/L) in PBS/CH_3CN (v/v, 7/3, pH 2–8 process.) (b) The change trend of BSL (10 μmol/L) fluorescence spectrum in PBS/CH_3CN (v/v, 7/3, pH 2–8 process.) (c) Curve relationship between fluorescence intensity ratio (F_{525}/F_{677}) and pH. (d) The fluorescence intensity ratio showed a linear relationship with a certain pH range. (λ_{ex} = 445 nm, slit: 10 nm/5 nm).

small damage and high detection sensitivity for biological samples [34]. Therefore, it is necessary to develop fluorescent probes with emission wavelengths in the NIR and large Stokes shifts to detect the small pH changes in lysosomes.

Spiropyran, as a photochromic material, is prone to isomerization from spiral-ring to π-conjugated structure under UV irradiation. Benzothiazole dyes are widely used in fluorescent probes because of their high fluorescence quantum yield, superior photostability and potentially large Stokes shift.

Herein, we designed and synthesized a new ratio NIR fluorescent probe **BSL** based on spiropyran skeleton as pH sensitive switch (Scheme 1). The probe **BSL** retains the spiropyran structure at a pH (beyond 6), so it only shows the emission (525 nm) of enol structure. Therefore, there is almost without NIR fluorescence emission in neutral and alkaline environments. Only under acidic conditions, spiropyran ring structure extended to π-conjugated structure and the transformation from enol (525 nm) to ketone (677 nm) structure occurred simultaneously under the ESIPT effect under photoexcitation, and the NIR fluorescence was accompanied with a significant Stokes shift (232 nm). Thankfully, **BSL** has a pK_a of 5.08 ± 0.84, while lysosome pH is typically 4.5–5.0, providing a favourable match. In the subsequent co-localization experiments, it was also proved that the probe could target in the lysosome and had excellent targeting ability.

The probe **BSL** was synthesized according to the synthesis steps in Figs. S1-S4 (Supporting information) in the supporting information. We studied the UV absorption and fluorescence spectra of phosphate buffer solution of probe **BSL** at different pH values. As shown in Fig. 1a, the UV absorption of the probe changes greatly in the process of pH 2–8. When the probe is in the solution of pH 2, it has the maximum absorption peak at 445 nm, and when the solution pH increases to 8, it has a small absorption peak at 445 nm. When the pH value gradually decreased from 8 to 2, the absorption peak at 445 nm increased rapidly, and the solution color gradually changed from colorless to yellow. Taking 445 nm as the characteristic absorption peak of the probe, when we excited the probe with 445 nm, the fluorescence intensity at 677 nm increased rapidly in the process of pH decreasing from 8 to 2, and the fluorescence intensity at 677 nm reached the maximum value at pH 2, while the fluorescence intensity at 525 nm gradually decreased (Fig. 1b). When the pH value is 2, the fluorescence at 525 nm reached the lowest point, ratiometric fluorescence changes under single wavelength excitation were achieved. Through the fluorescence curve fitting (Fig. 1c), the pK_a of the probe was calculated to be 5.08 ± 0.84, indicating that the probe could respond well to a wide range of pH, and there was a good linear relationship between the fluorescence intensity ratio and pH of the probe at pH 3.5–6 (Fig. 1d). We also studied the photostability (Fig. S5 in Supporting information) and pH reversibility (Fig. S6 in Supporting information) of the probe BSL, indicating that the probe has superior photophysical properties .

We also measured the probe's fluorescence response to various heavy metal ions and biomolecules present in organisms, as shown in Fig. S7 (Supporting information). The experimental results show that the probe **BSL** has high selectivity for pH.

The response mechanism of **BSL** and H^+ was verified by NMR titration experiment. As shown in Scheme 2, around 3.3 is the characteristic peak of hydrogen on the methylene group directly connected to the indole nitrogen. When reacting with H^+, a strong chemical shift from 3.3 to 4.8 was generated, indicating that the probe changed from tertiary amine structure to ammonium salt structure, which proved that the spirane structure of probe **BSL** was destroyed under the action of H^+. At the same time, the hydrogen in the aromatic ring region also changed greatly, which may be due to the change of the spatial structure of the probe. Under the action of H^+, **BSL** gradually extended into a plane structure, resulting in small changes in hydrogen in other positions. These experimental phenomena are almost in agreement with our initial conjecture.

The biocompatibility of the probe **BSL** was estimated by MTT assay before cell experiments, as shown in Fig. S8 (Supporting information). When the probe concentration was gradually increased to 40 μmol/L and the HeLa cell viability was close to 90% under 12 h co-incubation conditions, indicating that the toxicity of the probe was negligible.

Next, we studied the sensitivity of probe **BSL** to intracellular pH fluctuations. HeLa cells were treated with nigericin and KCl to stabilize the cell pH. The cells were co-incubated with buffer solutions of 4.5, 5.5, 6.5 and 7.4 for 20 min, and then washed with corresponding pH buffer solution for confocal imaging. As shown in Fig. 2, with the gradual increase of pH from 4.5 to 7.4, the fluorescence in the red channel gradually weakened, while the fluorescence in the blue channel gradually increased, which was consistent with the ratio fluorescence trend *in vitro*.

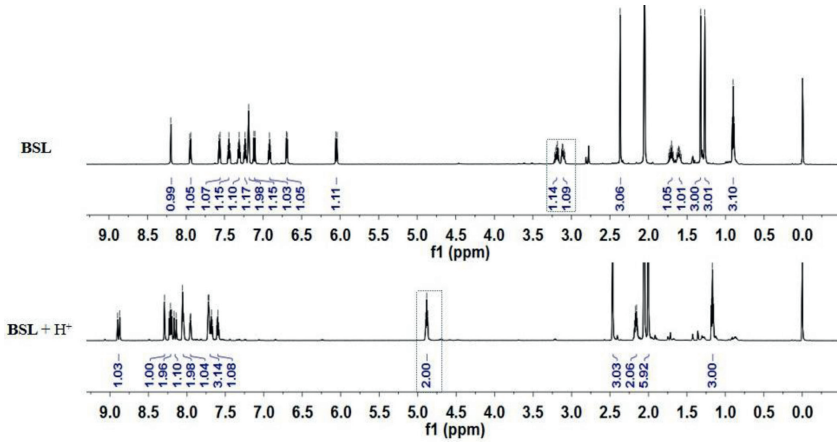

Scheme 2. ^{1}H NMR spectra in CD_3COCD_3-d_6 (aromatic and aliphatic regions) of probe BSL before (upper row) and after the addition of 1 equiv. of DCl (lower row).

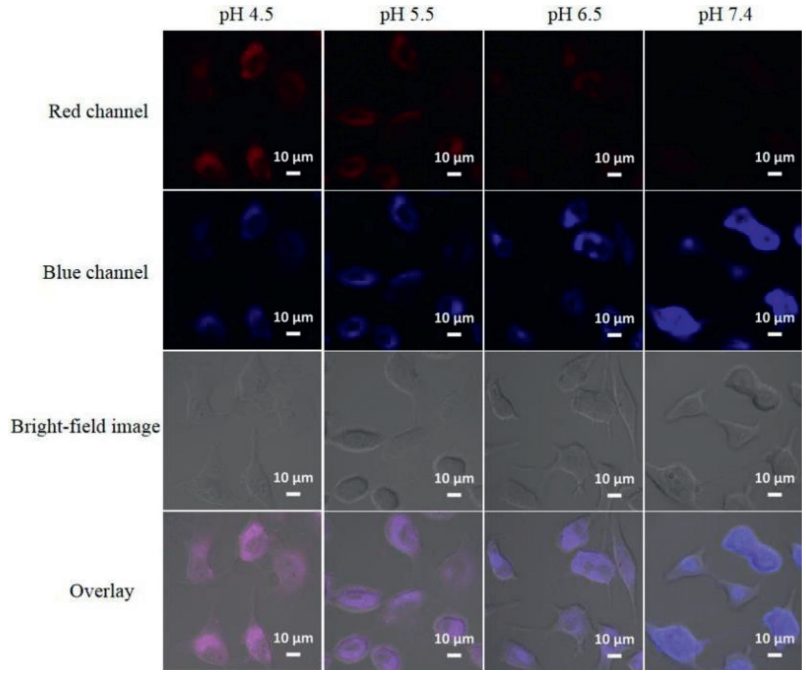

Fig. 2. Fluorescent imaging of HeLa cells with different pH cytoplasm. HeLa cells were pretreated with nigericin (10 μmol/L) and KCl (1 mmol/L) in different pH buffers to stabilize cell pH. HeLa cells were first incubated with buffers of different pH values for 30 min and then treated with BSL (10 μmol/L) for 15 min. Red channel: $\lambda_{ex} = 405$ nm, $\lambda_{em} = 640–700$ nm; Blue channel: $\lambda_{ex} = 405$ nm, $\lambda_{em} = 500–560$ nm. Scale bars = 10 μm.

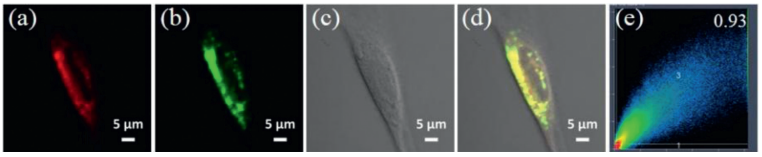

Fig. 3. Confocal microimaging of HeLa cells co-incubated with BSL (10 μmol/L) and Lyso-Tracker green (1 mmol/L) for 20 min: (a) the green channel imaging; (b) the red channel imaging; (c) bright-field imaging; (d) overlay imaging; (e) Pearson correlation coefficient of red channel and green channel. Red channel: 670 ± 30 nm for BSL ($\lambda_{ex} = 405$ nm); green channel: 510 ± 30 nm for Lyso-Tracker-Green ($\lambda_{ex} = 488$ nm). Scale bars = 5 μm.

When pH was 7.4, the fluorescence intensity did not disappear completely, and the red fluorescence showed small dot distribution, consistent with lysosome morphological characteristics. We suspected that the probe might have the potential lysosome localization ability, because the pH in the lysosome was 4.5–5.0, and the probe opened the ring to release the red fluorescence under acidic conditions after entering the cell. To confirm our hypothesis, **BSL** was co-located with, a commercial lysosomal dye. As shown in Fig. 3, probe **BSL** and Lyso-Tracker green were co-incubated with HeLa cells for 15 min. The red channel of probe **BSL** overlapped well with the green channel of Lyso-Green (Pearson's correlation coefficient were 0.93). This finding suggests that the red signal of probe **BSL** originates in lysosomes.

It has been reported that high concentration of NH_4Cl solution can effectively increase cytoplasmic pH value [35]. In order to verify the real-time pH monitoring ability of **BSL** in the cell physiological environment, HeLa cells were co-incubated with NH_4Cl (2 mL, 5 mmol/L) solution for 30 min and then co-incubated with

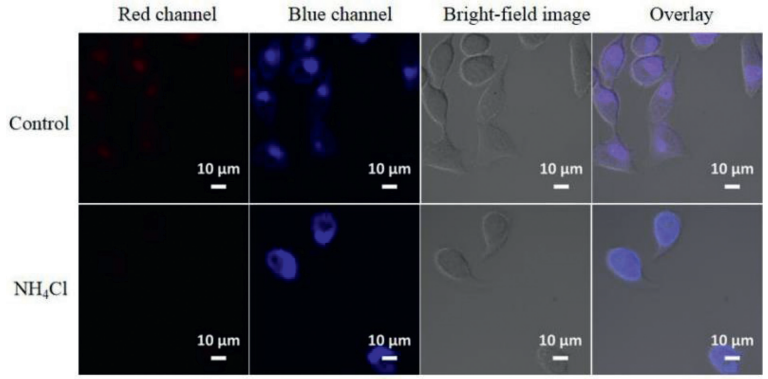

Fig. 4. Fluorescence imaging of HeLa cells treated with and without NH_4Cl. In the control group, HeLa cells were treated with normal saline (5 mmol/L) for 30 min and then incubated with BSL (10 μmol/L) for 15 min. The experimental group was treated with NH_4Cl (5 mmol/L) and then incubated with BSL (10 μmol/L) for 15 min. Red channel: $\lambda_{ex} = 405$ nm, $\lambda_{em} = 640–700$ nm; Blue channel: $\lambda_{ex} = 405$ nm, $\lambda_{em} = 500–560$ nm. Scale bars = 10 μm.

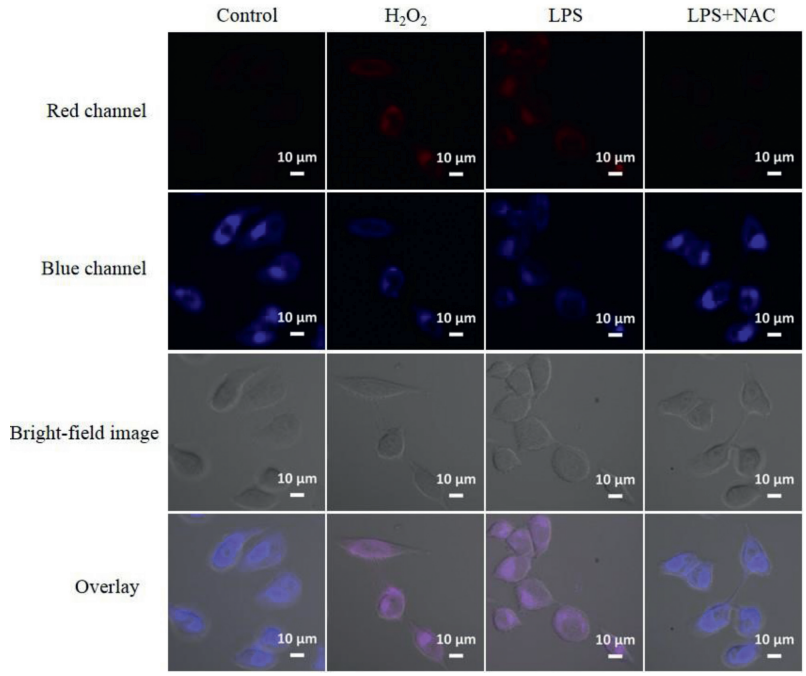

Fig. 5. Fluorescence imaging of pH changes induced by oxidative stress. In the control group, HeLa cells were incubated with BSL (10 μmol/L) for 15 min. HeLa cells were pre-incubated with H_2O_2 (0.1 mmol/L), LPS (10 μg/mL) and LPS (10 μg/mL) + NAC (1.0 mmol/L) in H_2O_2 group, LPS and LPS+NAC group for 30 min, and then co-incubated with BSL (10 μmol/L) for 15 min, respectively. Red channel: $\lambda_{ex} = 405$ nm, $\lambda_{em} = 640–700$ nm; Blue channel: $\lambda_{ex} = 405$ nm, $\lambda_{em} = 500–560$ nm. Scale bars = 10 μm.

the probe for 15 min for confocal microscopic imaging. As shown in Fig. 4, the fluorescence intensity in the red channel of the NH_4Cl treated group was significantly lower than that in the control group, while the fluorescence intensity in the blue channel was significantly stronger than that in the untreated control group. Experimental results showed that the cytoplasmic pH increased significantly after NH_4Cl treatment.

Since reactive oxygen species increased during oxidative stress, we wanted to know whether intracellular oxidative stress was accompanied by changes in cell pH. We designed experiments to demonstrate pH changes during oxidative stress in living cells (Fig. 5). HeLa cells incubated with **BSL** were used as the control group to verify whether H_2O_2 treatment could cause cell pH decline through the cell group treated with H_2O_2. As shown in Fig. 5, compared with the control group, after H_2O_2 treatment, fluorescence in the red channel was enhanced while fluorescence in the blue channel was significantly weakened. This result indicated that the intracellular pH was significantly decreased after H_2O_2 treatment. HeLa cells were pretreated with lipopolysaccharide (LPS, an oxidative stress inducer) and then co-incubated with BSL. As shown in Fig. 5, we can see that the fluorescence intensity in the red channel is significantly higher than that in the control group, while that in the blue channel is lower than that in the control group. To further explain that LPS induced ROS production and reduced cell pH, LPS and NAC (*N*-acetylcysteine, a GSH precursor, a reducing substance) were co-incubated with HeLa cells and then incubated with **BSL**. As shown in Fig. 5, compared with the LPS group alone, the fluorescence of red channel in LPS+NAC group was significantly decreased, while the fluorescence of blue channel was increased. This revealed that intracellular pH decreased during oxidative stress, and NAC, as a reducing substance, could also indirectly participate in intracellular pH changes.

In conclusion, herein introduces a new NIR fluorescent probe **BSL**, which has characteristic of excellent performance in living cell. Under the activation of pH, the ratio fluorescence signal changes under single wavelength excitation were realized through molecular isomerization. The probe **BSL** has superior sensitivity and selectivity to pH and has sensitive response to intracellular pH.

By simulating the intracellular oxidative stress, it was found that the cell pH changed with the change of cellular oxidative stress level. In order to further study oxidative stress disease diagnosis provides a powerful tool.

Declaration of competing interest

The authors declare that they have no known competing financial interests or personal relationships that could have appeared to influence the work reported in this paper.

Acknowledgments

We thank the National Natural Science Foundation of China (No. 22074084), One Hundred People Plan of Shanxi Province, Shanxi Province "1331 Project" Key Innovation Team Construction Plan Cultivation Team (No. 2018-CT-1), Research Project Supported by Shanxi Scholarship Council of China (No. 2022-002), Shanxi Province Foundation for Returness (No. 2017-026), Shanxi Collaborative Innovation Center of High Value-added Utilization of Coal-related Wastes (No. 2015-10-B3), the Shanxi Province Foundation for Selected (2019), Innovative Talents of Higher Education Institutions of Shanxi, Scientific and Technological Innovation Programs of Higher Education Institutions in Shanxi (No. 2019L0031), Key R&D Program of Shanxi Province (No. 201903D421069), the Shanxi Province Science Foundation (No. 201901D111015), Key R&D and Transformation Plan of Qinghai Province (No. 2020-GX-101), Graduate Innovation Project of Shanxi Province and Scientific Instrument Center of Shanxi University (No. 201512).

Supplementary materials

Supplementary material associated with this article can be found, in the online version, at doi:10.1016/j.cclet.2022.107818.

References

[1] J.R. Casey, S. Grinstein, J. Orlowski, Nat. Rev. Mol. Cell Biol. 11 (2010) 50–61.
[2] B. Dong, W. Song, Y. Lu, et al., Chem. Commun. 55 (2019) 10776–10779.
[3] Y. Wen, N. Jing, F. Huo, C. Yin, Analyst 146 (2021) 7450–7463.
[4] X. Zhang, F. Huo, Y. Zhang, et al., Analyst 147 (2022) 2470–2476.
[5] G. Song, D. Jiang, L. Wang, et al., Chin. Chem. Lett. 33 (2022) 339–343.
[6] B. Feng, Y. Zhu, J. Wu, et al., Chin. Chem. Lett. 32 (2021) 3057–3060.
[7] T. Zhang, F. Huo, W. Zhang, et al., Sens. Actuat. B 345 (2021) 130393–130400.
[8] Y. Wen, W. Zhang, T. Liu, et al., Anal. Chem. 89 (2017) 11869–11874.
[9] M. Fang, R. Adhikari, J. Bi, et al., J. Mater. Chem. B 5 (2017) 9579–9590.
[10] Y. Sun, X. Zhou, L. Sun, et al., Chin. Chem. Lett. 33 (2022) 4229–4232.
[11] T. Nishi, M. Forgac, Nat. Rev. Mol. Cell Biol. 3 (2002) 94–103.
[12] X. Liu, Y. Su, H. Tian, et al., Anal Chem. 89 (2017) 7038–7045.
[13] Y. Yue, F. Huo, S. Lee, et al., Analyst 142 (2017) 30–41.
[14] L. Chen, J. Li, Z. Liu, et al., RSC Adv. 3 (2013) 13412–13416.
[15] S. Park, J. Hyun, I. Shin, Chem. Sci. 10 (2019) 56–66.
[16] C. Chen, L. Zhou, W. Liu, W. Liu, Anal. Chem. 90 (2018) 6138–6143.
[17] Z. Dong, Q. Han, Z. Mou, et al., J. Mater. Chem. B 6 (2018) 1322–1327.
[18] P. Swietach, S. Wigfield, P. Cobden, et al., J. Biol. Chem. 283 (2008) 20473–20483.
[19] Q. Wan, S. Chen, W. Shi, et al., Angew. Chem. Int. Ed. 53 (2014) 10916–10920.
[20] T. Fukuda, L. Ewan, M. Bauer, et al., Ann. Neurol. 59 (2006) 700–708.
[21] R. Balaban, S. Nemoto, T. Finkel, Cell 120 (2005) 483–495.
[22] T. Fukai, M. Ushio-Fukai, Cell 9 (2020) 1849–1865.
[23] M. Reth, Nat. Immunol. 3 (2002) 1129–1134.
[24] J. Ge, K. Zhang, L. Fan, et al., Analyst 144 (2019) 4288–4294.
[25] A. Lieberman, R. Puetollano, N. Raben, et al., Autophagy 8 (2012) 719–730.
[26] J. Han, K. Burgess, Chem. Rev. 110 (2010) 2709–2728.
[27] D. Ellis, R.C. Thomas, Nature 262 (1976) 224–225.
[28] B. Lin, L. Fan, J. Ge, et al., Analyst 143 (2018) 5054–5060.
[29] J. Hou, W. Ren, K. Li, et al., Chem. Soc. Rev. 46 (2017) 2076–2090.
[30] C. Benitez-Martin, J. Guadix, J. Pearson, ACS Sens. 5 (2020) 1068–1074.
[31] B. Lin, L. Fan, Y. Zhou, et al., J. Mater. Chem. B 8 (2020) 10586–10592.
[32] L. Shi, S. Yang, H. Hong, et al., Anal. Chim. Acta 1094 (2020) 122–129.
[33] Z. Xu, S. Han, C. Lee, et al., Chem. Commun. 46 (2010) 1679–1681.
[34] T. Ren, W. Xu, W. Zhang, et al., J. Am. Chem. Soc. 140 (2018) 7716–7722.
[35] K. Joong, H. Ho, K. Myung, J. Am. Chem. Soc. 135 (2013) 17969–17977.